Conditions for Thermal Circulation in Urban Street Canyons

Ann Dallman , S. Magnusson , R. Britter , L. Norford , D. Entekhabi , H.J.S. Fernando

PII: S0360-1323(14)00150-4

DOI: 10.1016/j.buildenv.2014.05.014

Reference: BAE 3710

To appear in: *Building and Environment*

Received Date: 24 March 2014

Revised Date: 16 May 2014

Accepted Date: 18 May 2014

Please cite this article as: Dallman A, Magnusson S, Britter R, Norford L, Entekhabi D, Fernando HJS, Conditions for Thermal Circulation in Urban Street Canyons, *Building and Environment* (2014), doi: 10.1016/j.buildenv.2014.05.014.

Conditions for Thermal Circulation in Urban Street Canyons

Ann Dallman[1], S. Magnusson[2], R. Britter[3],
L. Norford[4], D. Entekhabi[2], and H.J.S. Fernando[1]

[1] Department of Civil & Environmental Engineering & Earth Sciences, University of Notre Dame, Notre Dame, IN 46556, USA

[2]Department of Civil and Environmental Engineering, Massachusetts Institute of Technology, Boston, MA 02139, USA

[3]Department of Urban Studies and Planning, Massachusetts Institute of Technology, Boston, MA 02139, USA

[4]Department of Architecture, Massachusetts Institute of Technology, Boston, MA 02139, USA

Corresponding Author:
A. Dallman
ardallm@gmail.com

Under conditions of low background winds and high solar radiation, non-uniform heating of building walls and the ground in an urban street canyon may induce thermally driven circulation that competes with inertially driven circulation due to overlying winds. These two types of circulation were studied using a field experiment, wherein a mock building canyon constructed with two rows of north-south aligned shipping containers were subjected to natural differential wall heating and overlying winds of varying magnitude. The site was carefully instrumented, and the measurements and flow visualization were conducted over nine days with varying environmental conditions. A buoyancy parameter, $B = (g\alpha\Delta TH)/({u_0}^2[1 + (H/L)^2])$, where $g\alpha\Delta T$ is the horizontal anomaly of buoyancy arising from differential heating of canyon walls, H the canyon height, L the canyon width and u_0 the background velocity, was derived to demarcate thermal and inertial circulation regimes. When $B < B_c$, where $B_c(\approx 0.05)$ is a critical value, the inertial circulation prevails, and the canyon velocities scaled by u_0 are approximately constant. When $B > B_c$, the thermal circulation becomes important and at $B \gg B_c$, the

flow is expected to be independent of u_0. An intermediate regime is found in the proximity of B_c, where the scaled velocity is dependent both on overlying flow and buoyancy effects.

Keywords: atmospheric flows, street canyon, urban canyon, buoyancy, thermal effects, dynamical regimes

1. Introduction

Thermally driven flow induced by solar heating of street canyons is an important topic because of its implications in building design, pedestrian comfort, air quality in urban canyons and emergency response planning [1-3]. Understanding of such flows is particularly important in light of recent policy emphasis on urban designs with environmentally friendly and energy efficient buildings [4-6]. Street canyons are in the lowest layer of the urban atmosphere (i.e., urban canopy layer) that exchanges heat and momentum between the ground and the rest of the atmosphere, and hence are critical elements in building and urban flow modeling and conceptual models for urban air quality planning [7-9]. The literature on urban street canyon flows and dispersion is voluminous, but only a few deals with thermal effects in canyons [10-12] and even less studies have dealt with non-uniform heating. The case of non-uniform heating has mainly been studied using wind-tunnel experiments [13,14] and numerical models [15-18], but very few field-scale studies have been reported although such studies are imperative for understanding of high Reynolds-number flows [19]. Obtaining insights on flow in actual urban canyons is difficult, given the spatial complexity of heating patterns (e.g., sensitivities to the orientation with respect to the sun, internal reflection of radiation), street traffic [20], and intricate flow morphologies (building facades, windows and balconies). These intricacies cause three-dimensional flows of multiple length and time scales [21,22]. While studies with such complexities are certainly important as they represent real situations, it is also useful to study urban canyon flows outdoors using more idealized geometries. Such real-life, high-Reynolds number experiments help delineate flow physics and fundamental scaling laws while providing

benchmark data for numerical modeling. This was the aim of the original Mock Urban Setting Test, MUST [23-25] dealing with 'man-sized' idealized street canyons, which was a source of inspiration for the present study.

To this end, a mock street canyon was constructed with two rows of shipping containers aligned in the north-south direction (i.e., canyon walls face the sun during certain phases of the diurnal cycle) and was appropriately instrumented with sonic anemometers, weather stations, and thermocouples attached to the building surfaces. The canyon circulation was studied under varying environmental conditions, and the effect of buoyancy was analyzed. Considering that this is the first controlled field attempt, the experimental design called for a simplified case of naturally heated walls but without appreciable thermal contributions from the ground surface, with the hope that the extension of this work will encompass such cases [26]. Section 2 presents theoretical considerations in order to determine the conditions for thermal or inertial dominance in a 2D canyon, which is the focus of this study. The experimental setup is described in Section 3, with general results in Section 4. A classification of flow regimes based on a dimensionless buoyancy parameter is discussed in Section 5, and conclusions are given in Section 6.

2. Theoretical considerations

Consider flow past an idealized two-dimensional street canyon, with a characteristic background velocity u_0, as shown in Fig. 1(a). The flow induced within the canyon for this case is inertially driven with vertical and horizontal velocity scales w_m and u_m, respectively. Assuming the skimming (or transition between skimming and wake interference) flow regime [19,27], the horizontal (u) and vertical (w) velocities in the canyon can be related to each other according to the continuity equation as $u/L \approx \beta\, w/H$, where $\beta \sim O(1)$ is a constant. For mechanically driven flow (denoted by subscript m), $u \sim u_m \sim u_0$, this becomes

$$\beta\, w_m/H \approx u_m/L \sim u_0/L, \tag{2.1}$$

and experimental results in Section 5 show that $\beta \approx 1$ for both inertially and thermally driven flows. If u_0 is sufficiently small and the walls of the canyon are differentially heated ($T_1 > T_2$), the thermally driven circulation is prevalent (Fig. 1(b)). Assuming that the flow is driven by the difference in wall temperature, with minimum contribution from the bottom surface energetics, the thermal circulation velocities $\underline{u_t} = (u_t,\ w_t)$ can be estimated using the vorticity ($\underline{\omega}$) equation with the baroclinic generation term. To the Boussinesq approximation, $D\underline{\omega}/Dt = \underline{\omega}.\nabla\underline{u} + \nabla \times b\underline{k} + \nu\,\nabla^2\underline{\omega}$, where $b(= g\alpha T)$ is the buoyancy acting in z direction (unit vector $\underline{k}$), g the gravitational acceleration, T the temperature, ν the kinematic viscosity, and $\alpha \approx 1/\bar{T}$ the thermal expansion coefficient where $\bar{T}$ is the average temperature within the canyon. If the amplification of vorticity by vortex stretching ($\underline{\omega}\,.\nabla\underline{u}$) and viscous diffusion of vorticity ($\nu\,\nabla^2\underline{\omega}$) are neglected, considering two dimensionality, and assuming Reynolds-number similarity of the flow, only the baroclinic generation of vorticity needs to be considered, $D\underline{\omega}/Dt \approx \nabla \times b\underline{k}$. Considering the y-component of vorticity (along the canyon axis, into the paper) and assuming quasi-steady flow, this becomes, in order of magnitude estimations,

$$\underline{u_t} \cdot \nabla\omega_y \sim -\frac{\partial b}{\partial x} \sim -\,g\alpha\frac{\partial T}{\partial x}\,, \tag{2.2}$$

where

$$\begin{aligned} \omega_y &\sim (\partial u/\partial z - \partial w/\partial x) \\ &\sim [\ u_t/H + w_t/L\ ] \\ &\sim [\ u_t/H + u_t/H\,(H/L)^2\ ] \\ &\sim (u_t/H)[1 + (H/L)^2], \end{aligned} \tag{2.3}$$

where $u_t/L \approx w_t/H$ has been used. Then (2.2) becomes

$$\underbrace{u_t \frac{\partial \omega_y}{\partial x}} + \underbrace{w_t \frac{\partial \omega_y}{\partial z}} \sim \underbrace{-g\alpha \frac{\partial T}{\partial x}},$$

$$\sim \frac{u_t}{L}\frac{u_t}{H}\left[1+\left(\frac{H}{L}\right)^2\right] \sim \frac{w_t}{H}\frac{u_t}{H}\left[1+\left(\frac{H}{L}\right)^2\right] \sim \frac{g\,\alpha\,\Delta T}{L}, \tag{2.4}$$

where $\Delta T = T_1 - T_2$. Thus, the scale for thermal circulation is

$$u_t \sim \left(\frac{g\,\alpha\,\Delta T\,H}{[1+(H/L)^2]}\right)^{1/2}. \tag{2.5}$$

When a mean flow and thermal circulation are both present, the latter could dominate when $u_t \gg u_m$,

$$B = \left(\frac{g\,\alpha\,\Delta T\,H}{{u_0}^2\,[1+(H/L)^2]}\right) \gg B_c\,, \tag{2.6}$$

where B_c is a critical value of the buoyancy parameter B. Note that the buoyancy parameter is nominally similar to the traditional bulk Richardson number defined for cavity flows [28], but in this case the B parameter is defined in terms of the horizontal buoyancy difference with inclusion of aspect ratio.

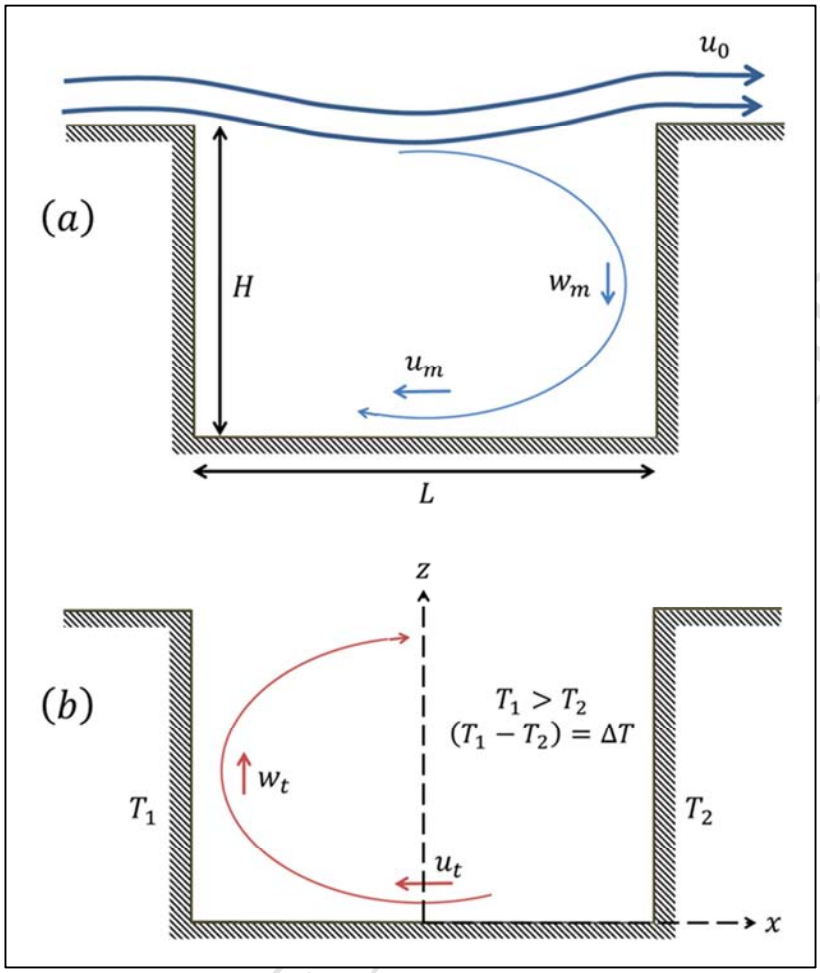

Fig. 1. (a) Inertially driven flow and (b) thermally driven flow in a canyon with aspect ratio $H/L \lesssim 1$.

3. Field Experiment Design and Site Characteristics

A simplified mock street canyon was constructed in a grassy field on the campus of Nanyang Technological University in Singapore at the location (1°21'22.5"N, 103°41'14.1"E). It consisted of two rows of shipping containers (2.5m in height and width; total length of each row 24.4m) aligned in the north-south direction with a 3.75m separation (Fig. 2), resulting in an aspect ratio of $H/L = 2/3$. Thus, according to the flow classification reviewed by Fernando et al. [19], it is in the transition from wake interference to the skimming flow regime, which is representative of typical cities [27]. The centerline of the canyon was instrumented with three-dimensional (3D) sonic anemometers (RM Young 81000) and

two-dimensional (2D) weather stations (Vaisala WXT520); the detailed locations of instruments are shown in Fig. 3. The sonic anemometers were placed within the canyon so that 3D flow and turbulence statistics could be measured, and the 2D weather stations were placed where flow was mostly two-dimensional (on the roof and near the ground) to obtain the mean circulation. Surface thermocouples (Campbell Scientific Type E, CS220) were mounted on the walls and roof. During selected periods, a fog machine (Antari Z Series) was used to visualize the flow. The data were recorded continuously during the experimental period (30 June to 9 July, 2012), and when the background flow was present, the flow was often from southeast/east. As shown in Fig. 3, there was a small local slope of the ground (0.04), but the thermally driven flow induced by the slope was estimated to be negligible. When the shipping containers were absent, no measurable directed slopes flows (upslope and downslope flows during day and night, respectively) were detected on the days of weak synoptic winds, showing that the local slopes play an insignificant role. In addition, the slope introduced a slight difference (0.25 m) in the mock buildings heights that caused the impingement characteristics on the windward wall to be different for the cases of westerly (i.e., west to east) and easterly flows. The differences of turbulence characteristics so introduced, however, were found to be unimportant as they were within the uncertainties introduced by natural variability and measurement errors. Some systematic differences were noted in turbulence measurements for the two cases when the approach flow was strong, at small B, but the differences were within the error bars. Thus, the main flows present are the background (synoptically driven) flow and the thermally driven flow in the urban canyon due to differential temperatures between the walls. The closest buildings to the mock canyon are approximately 22m to the east and 30m to the south, and their effects are minimal in distorting the flow around the mock street canyon. The overlying flows were directly measured so that local background flow information would be available. This precludes the necessity of considering flow distortions in the upstream face of the containers.

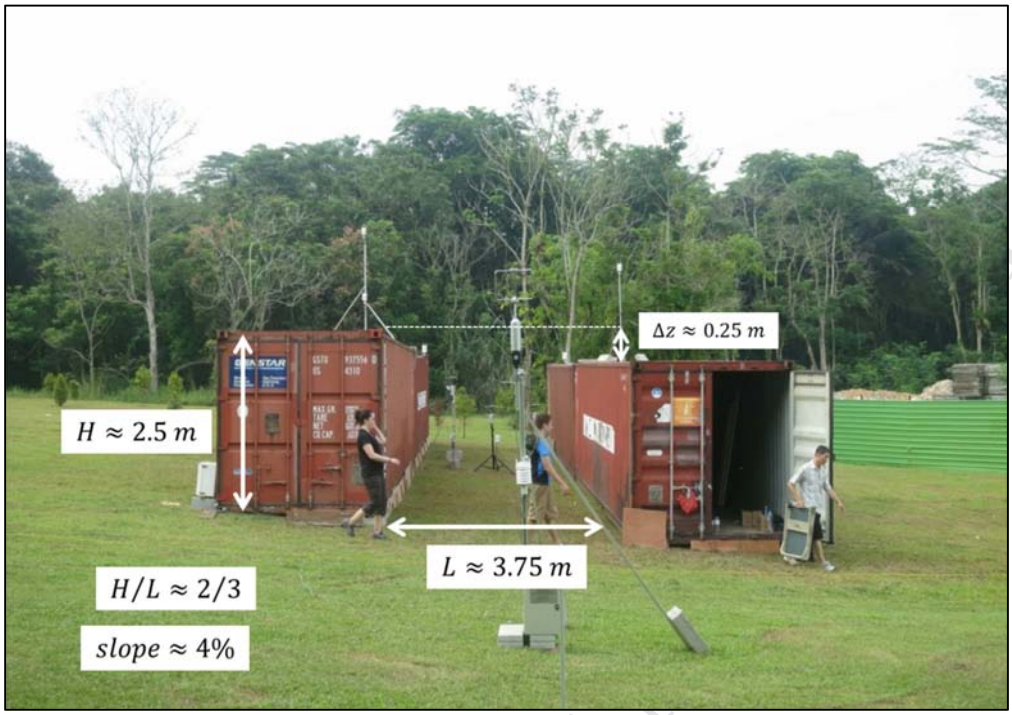

Fig. 2. Experiment setup, with aspect ratio shown. The view is looking towards north.

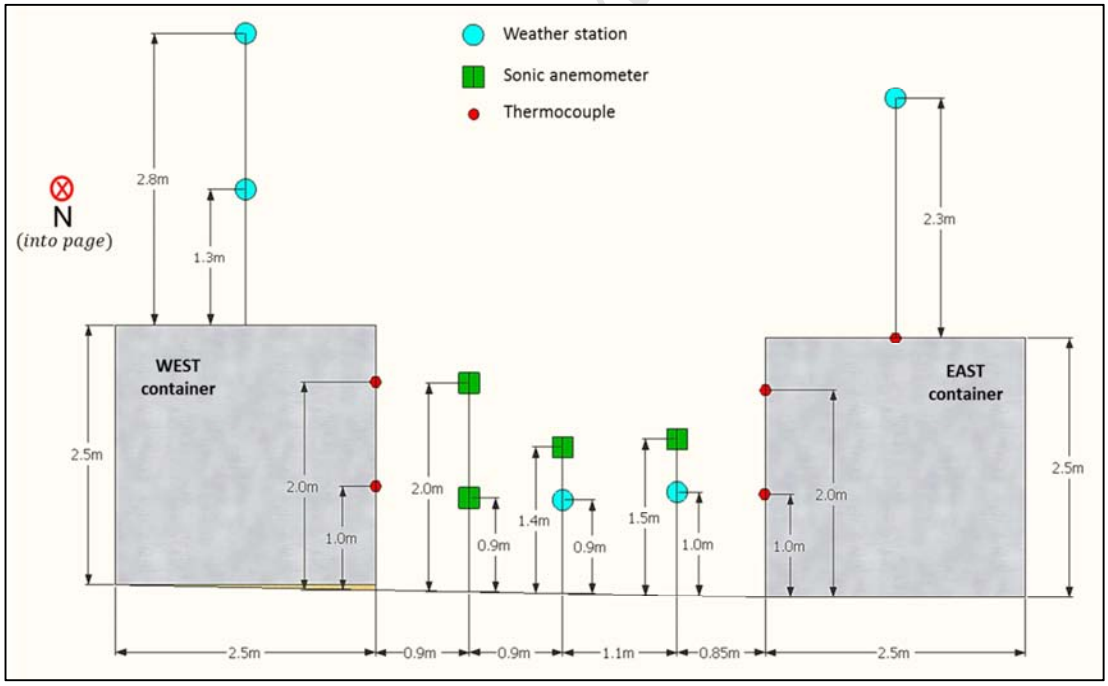

Fig. 3. Instrument layout at the experimental site. The locations of the instruments and elevations are shown.

4. Results

4.1. *General Observations*

During the summer, the weather in Singapore is hot (high solar radiation) and humid, and short periods of thunderstorms occur almost daily. Because the 'buildings' are made of steel, the thermal response is very rapid and the cloudy periods can be clearly discerned by a rapid drop of roof temperature. During such synoptically dominated periods, canyon circulation driven by the overlying flow dominates, overpowering the flow driven by local buoyancy gradients. The rest of the day, however, can be mostly characterized by high solar radiation and very low wind speeds (typically from southeast/east). In this case, the temperature differential that develops within the canyon drives the thermal flow, as has been observed and studied in numerical simulations [17,18]. The thermally driven flow was particularly apparent when the wind speeds were $u_0 < 1\ m/s$, where u_0 is the mean wind speed above the roof top at $z \approx 2H$.

4.2. *Flow visualization*

During selected periods of each day, a fog machine was used to visualize the canyon flow. The fog was produced using Antari FLR Low-Lying Fluid, which is a water-based composition, and ice. It can operate for approximately ten minutes at a time. Still photos from a video taken on July 2, 2012 at 12:27pm and 12:28pm LST are shown in Figs. 4 and 5, respectively. Simultaneously collected data are shown in Fig. 6(a,b), where the *u*- and *v*-components are from the ultrasonic anemometers and weather stations from a top view, and the *u*- and *w*-components are shown from the ultrasonic anemometers from an end view. It was cloudy during this time, and the temperature difference between the walls is $< 1℃$. In addition, the overlying flow is significant, resulting in a very low value of the buoyancy parameter ($B \approx 0.04$), so the flow is inertially driven (the critical value of B is discussed in Section 5). The visualization patterns and measured data match well.

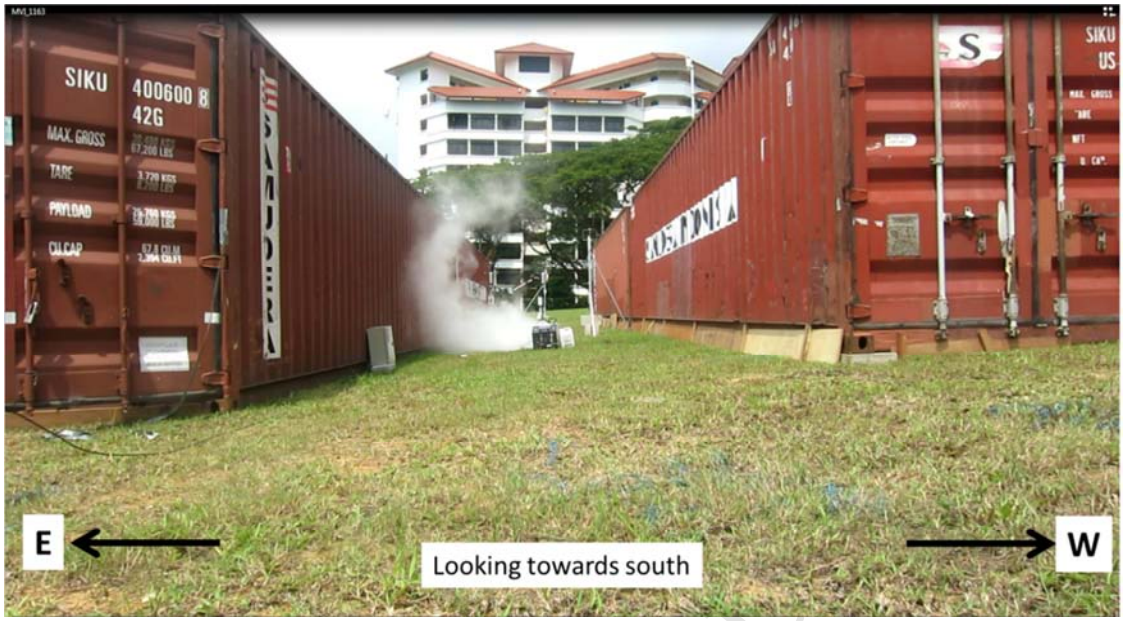

Fig. 4. Visualization on July 2, 2012 at 12:27 LST shows inertially driven flow forming a vortex, which is confirmed by concurrent data (Fig. 6(a)). The flow is in agreement with the $H/L \lesssim 1$ scenario.

Fig. 5. Visualization on July 2, 2012 at 12:28 LST shows a vortex being advected along the canyon due to a change in the background wind direction, which is confirmed by concurrent data (Fig. 6(b)).

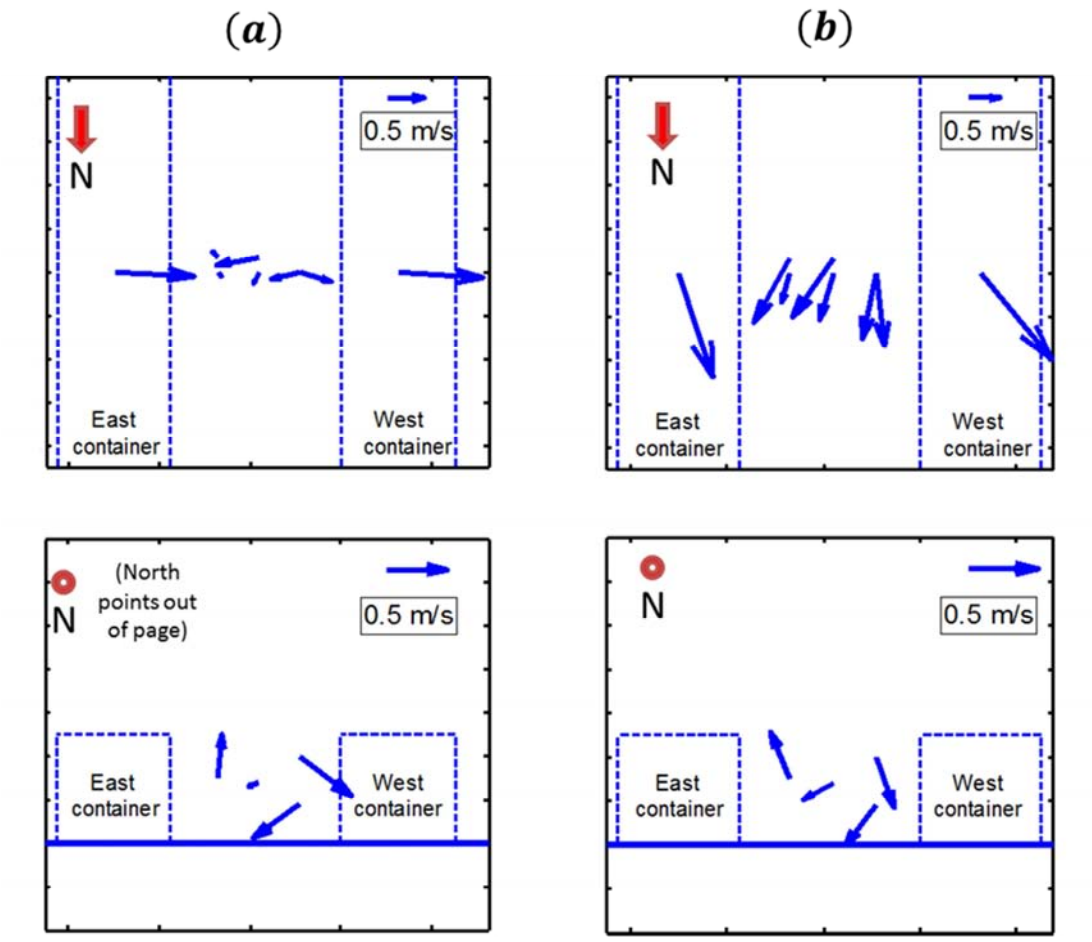

Fig. 6. (a) Wind vector data (30 sec averaged) during the video shot in Fig. 4 and (b) wind vector data during the video shot in Fig. 5 (top and end views in each figure).

4.3. *Data classification*

The data were classified into two groups for the case where the thermal and inertial circulations are in the same direction, which is considered 'assisting' [16]: (1) the mean flow was from west to east, or westerly ($270° \pm 15°$), and $T_1 \geq T_2$, (where T_1 and T_2 are the surface temperatures of the west and east walls, respectively), shown in Fig. 7(a); (2) the mean flow was east to west, or easterly ($90° \pm 15°$), and $T_1 \leq T_2$ (Fig. 7(b)). It has been found in previous numerical and laboratory studies [14,16,17] that 'opposing' cases, wherein the inertia and buoyancy effects promote circulations in opposite directions, cause a decrease in mean vorticity and possibly a second counter rotating vortex to form near the downwind

(warmer) wall. Instances of 'opposing' cases were observed in this study, but were not considered in the data analysis because of the complex flow pattern in the canyon, as evidenced in flow visualization studies. Such cases were difficult to delineate with only select measurement points in the field and could not be compared with the analysis presented in Section 2 wherein a single circulation cell is considered. Flow direction was limited to $\pm 15°$ from perpendicular to the canyon axis in order to avoid lateral channeling, as observed in Figure 5. A different analysis is required for such three dimensional cases [29].

If it is assumed that the velocity in the vortex is $1\,m/s$ and a fluid parcel approximately $0.1m$ from the wall and ground makes a complete circuit, the overturning time scale is $\tau \approx (2 * 2.3m + 2 * 3.55m)/(1\,m/s) = 11.7s$. Under normal circumstances, it would be prudent to use several overturns (say 6 circuits corresponding to ~1min) for averaging, but this was not possible because of the variability of flow at times of low wind speeds, particularly when the background wind direction changed over a time scale of a few minutes. Therefore, only 30-s averages of data (corresponding to ~3 overturns) were used, which would eliminate the low frequency variability. Only the two 'assisting' groups described above were of interest and hence analyzed. East to west (easterly) flow was more common, and there were about 50% more such cases than west to east cases. Periods of rain were excluded, but cloudy periods were included in the data analysis.

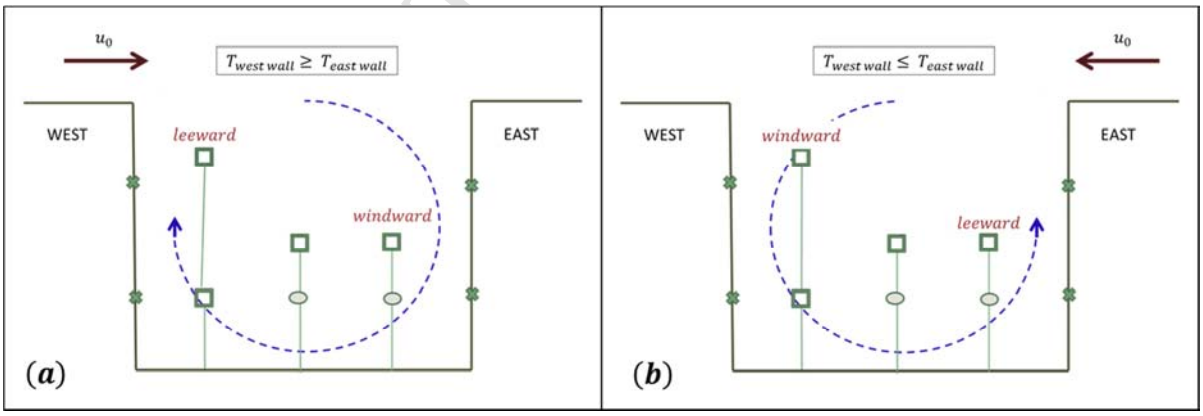

Fig. 7. (a) Westerly flow with either the same wall temperatures or west wall warmer. (b) Easterly flow with either same wall temperatures or east wall warmer.

5. Flow Regimes Classified by the Buoyancy Parameter

The field data is investigated to verify the assumption in (2.1), that is the in-canyon horizontal and vertical velocities are related by $u/L \approx \beta\, w/H$, where β is a constant. The measured mean horizontal velocity at the bottom center of the experimental canyon ($z/H \approx 0.36$) is plotted against the mean vertical velocity near the leeward (upstream) and windward (downstream) walls in Fig. 8; see Fig. 3 for the instrument placement. Conventional averaging techniques were used in calculating the mean and *rms* velocities, for example, according to Eq. (3) and (4) of Allegrini et al. [14]. 'Inertial' represents measurements for $B < B_c$, and 'thermal' is for $B > B_c$, and the evaluation of B_c (≈ 0.05) is discussed in Section 5.1. The best fit, $w = 0.65u$, is represented by the solid line. This matches the proposed vertical velocity scale, $w = (2/3)u$ almost exactly, and shows that $\beta \approx 1$ holds for both inertially and thermally dominated flows.

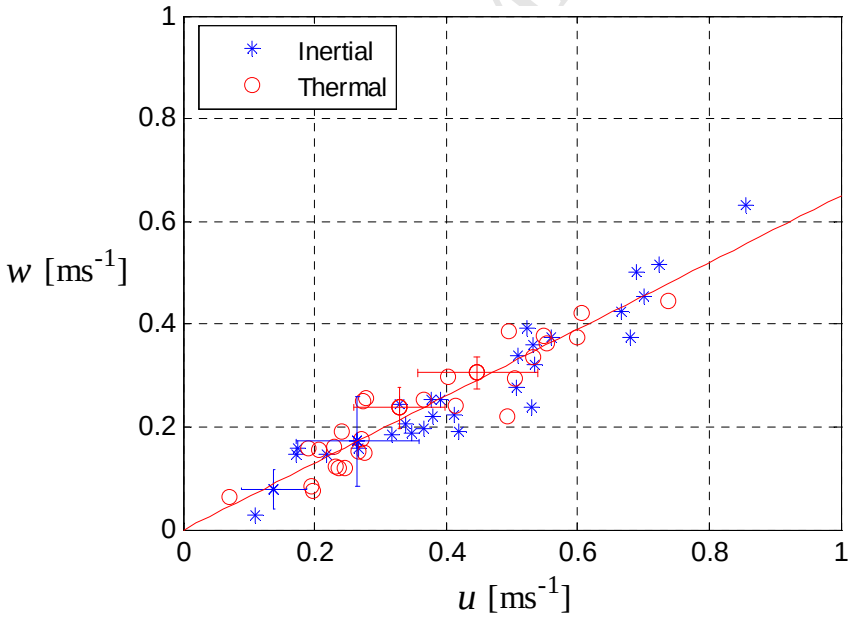

Fig. 8. Thirty second averages of in-canopy horizontal velocity (measured by the weather station at the bottom center of the canyon) vs. absolute value of the vertical velocity (taken as the average of the absolute vertical mean velocity measured by the sonics on the leeward and windward sides). For clarity, only a few representative error bars are shown.

5.1. *In-canopy horizontal velocity*

Based on (2.1), the horizontal velocity in the canyon for inertially driven flow should be proportional to u_0 while the vertical velocity, w_m, is dependent on the aspect ratio, H/L, and u_0. For purely thermally driven flow, based on (2.5), the horizontal velocity u_t should be a function of the buoyancy parameter B only, irrespective of u_0, and hence the following asymptotic forms can be proposed:

$$\frac{u}{u_0} \sim \begin{cases} \dfrac{u_m}{u_0} \approx \gamma_1 & B < B_c \\ \dfrac{u_t}{u_0} \approx \gamma_2 \, B^{1/2} & B \gg B_c \end{cases}, \tag{5.1a,b}$$

where γ_1 and γ_2 are constants. An intermediate regime is expected, where the flow is dependent on both the overlying flow and differential heating, and to the first order, using simple linear superposition, the resulting velocity can be represented as

$$\frac{u}{u_0} \approx \gamma_3 + \gamma_4 \, B^{1/2}, \tag{5.2}$$

where γ_3 and γ_4 are constants.

The measured scaled velocity as a function of B is shown in Fig. 9. Here the absolute value of the mean horizontal velocity measured by the Vaisala WXT520 located at the canyon center at a height of 0.9m ($z/H = 0.36$) was defined as the in-canopy horizontal velocity u. The above-canyon wind speed, u_0, was obtained from the top Vaisala on the west container (at $z/H = 2.12$) or the rooftop Vaisala on the east container (at $z/H = 1.92$) in order to represent the flow at $z/H \approx 2$. Data was bin averaged, and the error bars represent one standard deviation from the mean of all data points at a particular (logarithmically chosen) bin.

For small B values, the data are approximately constant with $u/u_0 \approx 0.42$. At higher B values, the scaled horizontal wind speed clearly increases with B, and the critical buoyancy parameter that demarcates the two regimes can be estimated as $B_c \approx 0.05$. Nevertheless, the data does not appear to reach the anticipated thermally dominated flow (5.1b). It is likely that the data in this region is still in transition between inertially and thermally dominated flows. The data were thus fitted to (5.2), and the

resulting fit, $u/u_0 = 0.40 + 0.60\ B^{1/2}$ for $B > 0.05$, is reasonable (dashed line). Whether the trend of increasing u/u_0 with increasing B will achieve the asymptotic form of $B^{1/2}$ or the flow transitions to another dynamical regime is yet to be determined, which needs to be investigated in future studies. It is noteworthy that Li et al. [10] used a LES code for a similar problem, but with ground heating only, and found that the in-canyon "recirculating" velocity increases without limit as heating is ramped up. RANS simulations of the same flow configuration considered here by Magnusson et al. [30] show that the asymptotic form (5.1b) is indeed achieved for $B > 50$.

A few studies have considered differential wall heating, for example, the numerical simulations of Park et al. [17] and wind tunnel experiments of Allegrini et al. [14], both of which were conducted with 2D street canyons of $H/L = 1$. To our knowledge, these are the only two studies with comparable aspect ratios and differential heating that can be compared with the present work, and their results are included in Fig. 9. While details vary, the pattern of nearly constant scaled velocity until a critical $B \approx 0.05$ is consistent in all studies. The data of Allegrini et al. for $B > 0.05$ (taken at $z/H \approx 0.2$) can be fitted to (5.2) as $u/u_0 = 0.29 + 0.21\ B^{1/2}$, which is not shown for clarity.

The agreement of laboratory and field results in the inertially dominated regime can be attributed to the high Reynolds number regime in both cases ($Re = u_0 H/\nu$ ~10^5 for the field and ~ 10^4 for laboratory experiments). Both are above the mixing transition $Re \sim 10^4$ [31,32] and hence they obey the Reynolds number similarity. Nevertheless, the Reynolds number in the thermal regime is much smaller in the laboratory experiments ($Re = uH/\nu \sim 10^3$) compared to the field (~ 10^4), and hence the laboratory experiments may not have achieved the Reynolds number similarity regime. In the latter, the results are expected to depend on the Reynolds number, and as postulated in the context of entrainment by Princevac et al. [32] the scaled results should differ from those of the high Reynolds number regime.

Also note that B values as high as 50 are unlikely to occur in reality, or at the least will be quite uncommon. The present results confirm (5.1a) for $B < B_c$, and for $B > B_c$ the u velocity can be described by (5.2) until the flow transitions to (5.1b) or some other asymptotic regime.

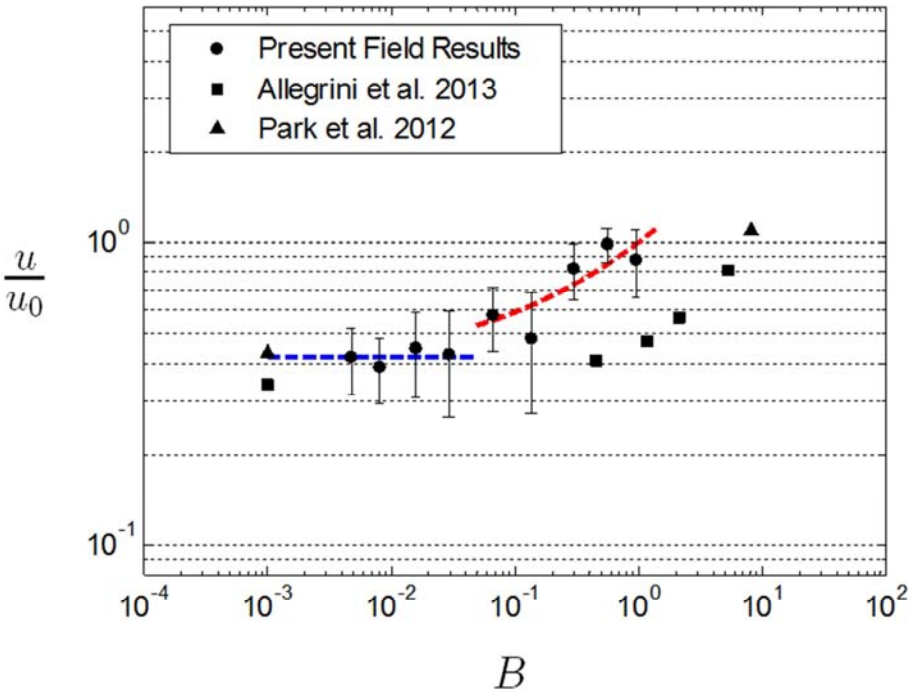

Fig. 9. Scaled canyon velocity vs. the buoyancy parameter (Wind tunnel data: courtesy of Dr. Jonas Allegrini).

5.2. *In-canopy rms velocities*

The *rms* turbulent velocities are important in reckoning the efficiency of canyon mixing and pollutant removal. To this end, the *u*-component of *rms* turbulent velocity σ_u scaled by u_0 is shown in Fig. 10 as a function of B. Only the sonic anemometers were used to evaluate *rms* values, given their higher (20Hz) frequency response (compared to 1Hz for the Vaisala weather stations, which were used to obtain mean circulation in Fig. 9). Owing to the nature of their placement, the *rms* velocities at the leeward and windward sides of the canyon were investigated. Analogous to the mean speed in Eq. (5.1), the results could be approximated by $\sigma_u/u_0 \approx 0.15$ for $B < B_c$ (i.e., B is unimportant), and for $B > B_c$, $\sigma_u/u_0 \approx 0.12 + 0.20\, B^{1/2}$ (i.e., transition regime). The wind tunnel results of Allegrini et al. [14] are also shown in Fig. 10, which confirms the trends of *rms* velocity.

Furthermore, the *v*- and *w*-components of rms turbulent velocities, σ_v and σ_w, scaled by σ_u are shown in Fig. 11. Given the constancy of the ratios, it is clear that σ_v and σ_w also follow the same dependence on B as σ_u; σ_v is the same as σ_u, while σ_w is slightly smaller. In all, the results show that,

even when u_0 is weak, there is still a mechanism for internal stirring and perhaps for the removal of pollutants from street canyons. The patterns of the dependence on *B* for thermally driven flow should be valid for other canyons of comparable aspect ratios ($H/L \lesssim 1$), that is for the cases where the structure of the flow in the canyon is the same (i.e., single recirculation cell with wake interference/skimming roughness).

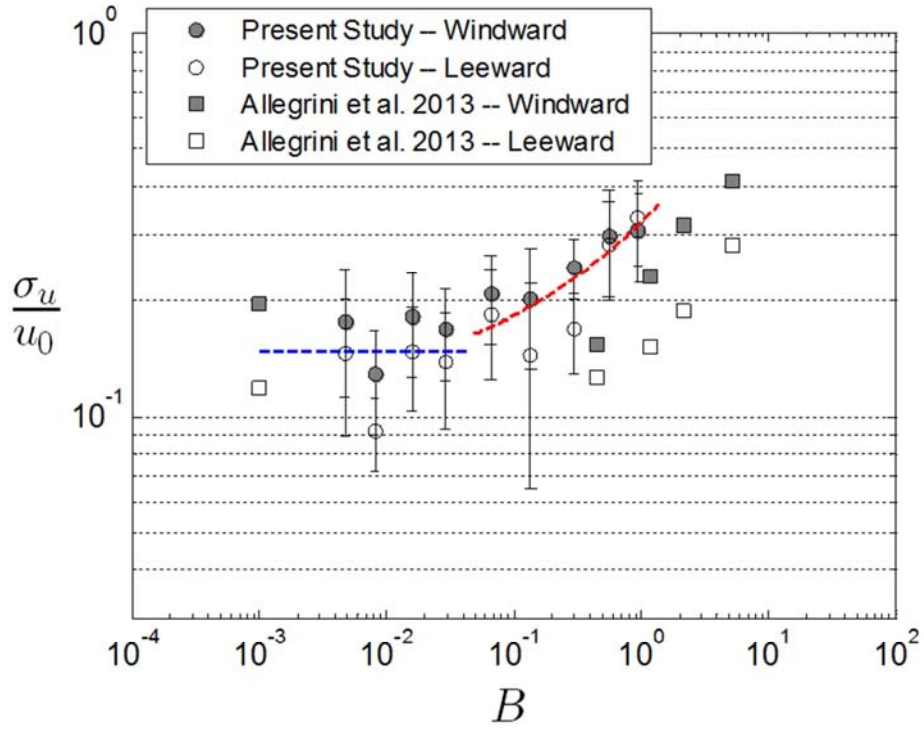

Fig. 10. Scaled east-west (normal to the canyon axis) *rms* velocity σ_u vs. the buoyancy parameter B from the sonics on the leeward and windward sides of the canyon (the average of both sonics located near the west container are shown).

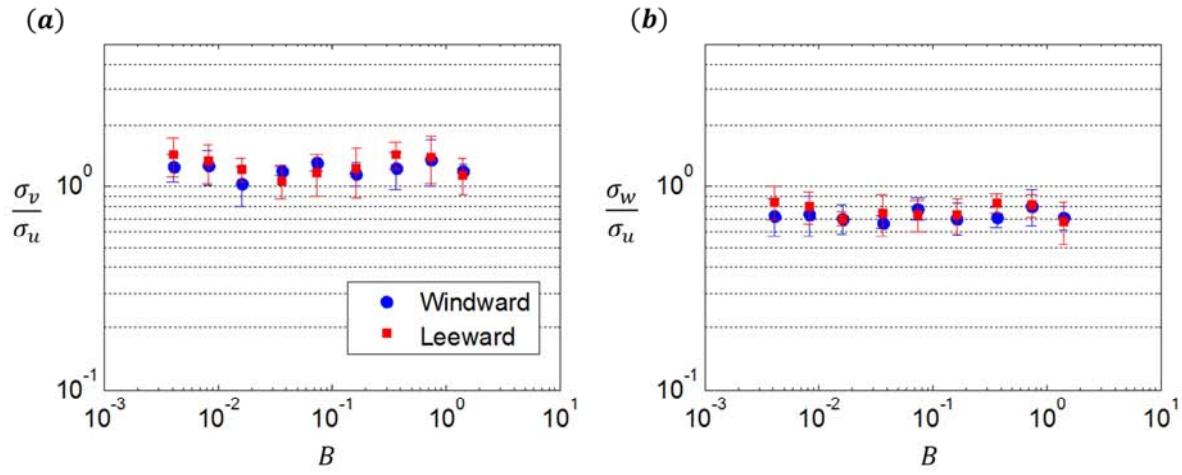

Fig. 11. Ratios of *rms* turbulent velocities (a) *v*- and *u*-components and (b) *w*- and *u*-components versus the buoyancy parameter *B*. Here σ_v is in the north-south direction (along canyon), and σ_w is vertically up.

5.3. *Further considerations*

In the present study, for $B > B_c$, the measured temperature difference ranged from 1-10°C. For dense urban areas with a mean building height $H = 10m$, canyon width $L = 10m$, wind speed $u_0 = 2m/s$, and average air temperature $\bar{T} = 300K$, a critical buoyancy parameter of $B_c = 0.05$ would require the wall temperature difference to be $\Delta T \approx 1.2°C$, which is fairly small and expected to be achieved in typical urban areas (e.g. see measurements in Fernando et al. [19]). For typical experiments in a wind tunnel, with $H = 0.1m$, $L = 0.1m$, $u_0 = 1m/s$, and $\bar{T} = 300K$, a critical buoyancy parameter of $B_c = 0.05$ would require $\Delta T \approx 30°C$, which is quite high (e.g., Allegrini et al. [14]) and leads to operational difficulties and failure of the Boussinesq approximation in the analysis. The Reynolds number of the flow considered in our field study is Re ~ 156,000, based on typical values $H = 2.5m$ and $u_0 = 1m/s$, which is well above the Reynolds-number similarity requirement. Castro and Robins [33] proposed a critical Re of 30,000 for bluff-body flows and based on the previous work of Dimotakis [31], Princevac et al. [32] proposed a critical Re of 10,000. The inertial regime studies of Allegrini et al. [14], with Re ~ 12,500, is in the vicinity of the latter critical Reynolds number, but Re ~ 1,000 in their thermal regime is clearly lower than the critical value. The inapplicability of the Boussinesq approximation and the differences in

the Reynolds number may in part explain the quantitative differences observed between laboratory and field studies at high B. Some of the above-mentioned difficulties can be alleviated by using water tunnel studies, because of the favorable physical properties. For $H = 0.1m$, $L = 0.1m$, $u_0 = 0.3m/s$, and $\bar{T} = 300K$, a critical buoyancy parameter of $B_c = 0.05$ would require $\Delta T \approx 2.8°C$, yielding a Reynolds number of about 30,000.

6. Conclusions

A new dimensionless (buoyancy) parameter, $B = \left(g\,\alpha\,\Delta T\,H\right)/({u_0}^2\,[1 + (H/L)^2]\,)$, was introduced to demarcate the regimes of inertially driven flow from the thermally driven flow in an idealized urban street canyon with differentially heated walls and overlying (synoptically driven) flow. For B less than a critical value, $B_c \approx 0.05$, the scaled mean horizontal velocity is $u/u_0 \approx 0.42$, indicating the unimportance of thermal effects. For $B \gg B_c$, the flow is expected to be dominated by thermal circulation and hence the normalized velocities to be dependent on $B^{1/2}$, although the present data could only achieve a clearly defined transition regime wherein both B and u_0 are important. Because realistic cases in the field will most likely have similar ranges of B as studied here, it is suggested that the intermediate regime, described by (5.2) for $B > B_c$ is appropriate to be included in thermal flow parameterizations in larger (meso) scale models. This signifies a mix of mechanically driven (u_m) and thermally driven (u_t) flows. Results from ongoing simulation studies, presented in Magnusson et al. [30], agree well with the asymptotic forms suggested herein.

The *rms* velocities followed suit, and it was found that for lower *B* the buoyancy is unimportant, and for higher *B* the overlying wind speed played a lesser role. When clear skies and low winds prevail, the pollutants can still be flushed out of urban canyons for $B > B_c$, which can be a useful result in planning for urban building canyons with high-pressure dominated climatology (e.g., Phoenix, Los Angeles and Houston). It should be noted, however, that the present work is applicable to cases of aspect ratios between ~ 0.3 to 1.2, where the flow within the canyon consists of a single circulation cell [30] and the

background and thermal flows are aiding. While it is a benchmark case for evaluating high Reynolds number numerical experiments, the present work calls for investigations of cases with complementary aspect ratios and opposing and oblique thermal and background flows. Efforts in the direction of using phenomenological models for urban building planning are rapidly growing [7]. In practice, however, possible benefits of thermally induced mixing within the canyon should be weighed against increased energy consumption for air conditioning due to (north-south) alignment of longer building facades to realize direct solar exposure.

Acknowledgments

This research was supported in part by the Singapore National Research Foundation through the Singapore-MIT Alliance for Research and Technology's (SMART) Center for Environmental Sensing and Modeling (CENSAM), the University of Notre Dame Professional Development Fund and the US National Science Foundation (CMG; Grant # 0934592). We are very grateful to Alex Toh, Shanshan Pan, and Casey Quandahl for their assistance with the experimental setup and Dr. Jonas Allegrini for providing original data of wind tunnel experiments.

References

[1] Ali-Toudert F, Mayer H. Numerical study on the effects of aspect ratio and orientation of an urban street canyon on outdoor thermal comfort in hot and dry climate. Build Environ 2006;41(2):94–108.

[2] Allegrini J, Dorer V, Carmeliet J. Analysis of convective heat transfer at building facades in street canyons and its influence on the predictions of space cooling demand in buildings. J Wind Eng Ind Aerod 2012;104-106:464-73.

[3] Kwak K-H, Baik J-J. Diurnal variation of NO_x and ozone exchange between a street canyon and the overlying air. Atmos Environ 2014;86:120-8.

[4] IPCC: Climate Change 2007: Mitigation of Climate Change. Contribution of Working Group III to the Fourth Assessment Report of the Intergovernmental Panel on Climate Change [Metz B, Davidson

OR, Bosch PR, Dave R, Meyer LA (eds)], Cambridge University Press, Cambridge, United Kingdom and New York, NY, USA, 2007;851pp.

[5] Bouyer J, Inard C, Musy M. Microclimatic coupling as a solution to improve building energy simulation in an urban context. Energ Buildings 2011;43(7):1549–59.

[6] Janssen WD, Blocken B, van Hooff T. Pedestrian wind comfort around buildings: Comparison of wind comfort criteria based on whole-flow field data for a complex case study. Build Environ 2013;59:547-62.

[7] Zhang Y, Gu Z. Air quality by urban design. Nature Geosci 2013;6:506.

[8] Doya M, Bozonnet E., Allard F. Experimental measurement of cool facades' performance in a dense urban environment. Energ Buildings 2012;55:42-50.

[9] Razak AA, Hagishima A, Ikegaya N, Tanimoto J. Analysis of airflow over building arrays for assessment of urban wind environment. Build Environ 2013;59:56-65.

[10] Li X-X, Britter RE, Koh T-Y, Norford LK, Liu C-H, Entekhabi D, Leung DYC. Large-Eddy Simulation of Flow and Pollutant Transport in Urban Street Canyons with Ground Heating. Bound-Lay Meteorol 2010;137:187-204.

[11] Li X-X, Britter RE, Norford LK, Koh T-Y, Entekhabi D. Flow and Pollutant Transport in Urban Street Canyons of Different Aspect Ratios with Ground Heating: Large-Eddy Simulation. Bound.-Lay. Meteorol. 2012;142:289-304.

[12] Allegrini J, Dorer V, Cameliet J. Buoyant flows in street canyons: Validation of CFD simulations with wind tunnel measurements. Build Environ 2014;72:63-74.

[13] Kovar-Panskus A, Moulinneuf L, Savory E, Abdelqari A, Sini J-F, Rosant J-M, Robins A, Toy N. A Wind Tunnel Investigation of the Influence of Solar-Induced Wall-Heating on the Flow Regime within a Simulated Urban Street Canyon. Water, Air, and Soil Poll: Focus 2002;2:555–71.

[14] Allegrini J, Dorer V, Carmeliet J. Wind tunnel measurements of buoyant flows in street canyons. Build Environ 2013;59:315-26.

[15] Basak T, Roy S, Krishna Babu S, Balakrishnan A. Finite element analysis of natural convection flow in a isosceles triangular enclosure due to uniform and non-uniform heating at the side walls. Intl J Heat Mass Trans 2008;51(17-18):4496-4505.

[16] Cai X-M. Effect of Wall Heating on Flow Characteristics in a Street Canyon. Bound.-Lay Meteorol 2012;142:443-67.

[17] Park S-B, Baik J-J, Raasch S, Letzel MO. A Large-Eddy Simulation Study of Thermal Effects on Turbulent Flow and Dispersion in and above a Street Canyon. J Appl Meteor Climatol 2012;51:829-41.

[18] Qu Y, Milliez M, Musson-Genon L, Carissimo B. Numerical study of the thermal effects of buildings on low-speed airflow taking into account 3D atmospheric radiation in urban canopy. J Wind Eng Ind Aerodyn 2012;104-106:474-483.

[19] Fernando HJS, Zajic D, Di Sabatino S, Dimitrova R, Hedquist B, Dallman A. Flow, turbulence, and pollutant dispersion in urban atmospheres. Phys Fluids 2010;22:051301-20.

[20] Louka P, Vachon G, Sini J-F, Mestayer G, Rosant J-M. Thermal Effects on the Airflow in a Street Canyon – Nantes '99 Experimental Results and Model Simulations. Water, Air, and Soil Poll: Focus 2002;2:351-364.

[21] Nakamura Y, Oke TR. Wind, Temperature and Stability Conditions in an East-West Oriented Urban Canyon. Atmos Environ 1988;22:2691-2700.

[22] Niachou K, Livada I, Santamouris M. Experimental study of temperature and airflow distribution inside an urban street canyon during hot summer weather conditions. Part II: Airflow analysis. Build Environ 2008;43:1393-1403.

[23] Biltoft CA. Customer Report for Mock Urban Setting test. Tech Rep 2001 WDTC-FR-01-121. U.S. Army Dugway Proving Ground, Dugway, Utah.

[24] Biltoft CA, Yee E, Jones CD. Overview of the Mock Urban Setting Test. Fourth Symposium on the Urban Environment, 2002, American Meteorological Society, Norfolk, Virginia, USA.

[25] Zajic D, Fernando HJS, Pardyjak E, Brown M. On Flows in Simulated Urban Canopies. Environ Fluid Mech 2014 In Press, DOI 10.1007/s10652-013-9311-6.

[26] Kim JJ, Baik JJ. Urban street-canyon flows with bottom heating. Atmos Environ 2001;35(20):3395–3404.

[27] Grimmond CSB, Oke TR. Aerodynamic Properties of Urban Areas Derived from Analysis of Surface Form. J Appl Meteorol 1999;38:1262-92.

[28] Strang EJ, Fernando HJS. Shear-induced mixing and transport from a rectangular cavity. J Fluid Mech 2004;520:23-49.

[29] Princevac M, Baik J-J, Li X, Pan H, Park S-B. Lateral channeling within rectangular arrays of cubical obstacles. J Wind Eng Ind Aerodyn 2010;98:377-85.

[30] Magnusson S, Dallman A, Entekhabi D, Britter R, Fernando HJS, Norford L. On Thermally Forced Flows in Urban Street Canyons. Environ Fluid Mech 2014; In Press, DOI 10.1007/s10652-014-9353-4.

[31] Dimotakis PE. The mixing transition in turbulent flows. J Fluid Mech 2000;409:69–98.

[32] Princevac M, Fernando HJS, Whiteman CD. Turbulent entrainment into natural gravity-driven flows. J Fluid Mech 2005;533:259-68.

[33] Castro IP, Robins AG. The flow around a surface mounted cube in uniform and turbulent streams. J Fluid Mech 1977;79:307-35.

Highlights

- We introduce a field experiment involving a mock urban street canyon
- We study the effect of non-uniform heating on the canyon circulation
- We introduce a new buoyancy parameter to delineate inertial and buoyancy dominated regimes
- Three dynamical flow regimes are proposed with clear evidence of the first two
- Laboratory data from the literature is also considered